



26 **Keywords:** urban flooding; resident travel behavior; agent-based model; dynamic exposure

27 **1. Introduction**

28 Storm flooding has become increasingly frequent and severe with the intensification of global
29 warming and the rising frequency of extreme weather events (*Dankers and Feyen, 2008*;
30 *Hammond et al., 2015*). Urban floods have become major natural disasters in many cities around
31 the world and have created serious threats to human life and social and economic activities (*Gain*
32 *et al., 2015*). Effectively coping with floods and their adverse effects is an important part of disaster
33 prevention and mitigation as well as disaster risk management (*Atta-Ur-Rahman, 2014*). Non-
34 engineering measures such as exposure assessment are currently the main way of managing urban
35 flooding risk (*Chen et al., 2015*). Exposure refers to the presence of people, livelihoods,
36 environmental services and resources, infrastructure, or economic, social, or cultural assets in
37 places that could be adversely affected by natural disasters (*IPCC, 2012*). Urban flood disasters
38 are caused by the adverse effects of heavy rain and other factors on the city system in certain
39 disaster-pregnant environments. These events consist of three parts: the disaster-causing factors,
40 the disaster-pregnant environment, and the disaster-bearing bodies (*Shi, 1996*).

41 Exposure has obvious dynamic characteristics because of the dynamic evolution of urban floods
42 and disaster-bearing bodies. Therefore, the characteristics of flood disasters and building
43 environments and the distribution of population and socio-economic resources are the key factors
44 for evaluating urban flood exposure. The methods for evaluating exposure to urban flooding at a
45 certain time or period vary due to changes in the disaster-bearing bodies, study areas, data
46 acquisition methods, etc. (*Röthlisberger et al., 2017*). Index-based methods are commonly used



47 for comprehensive exposure evaluation (*Mahe et al., 2005; Mansur et al., 2016; Guo et al., 2014*).

48 Statistical methods based on historical disaster data are also utilized (*Moel et al., 2011*).

49 With respect to spatial considerations, the currently implemented method for estimation of disaster
50 exposure adopts the administrative boundaries of socioeconomic data, which are organized as
51 research units (*Yin, 2009*). Consequently, natural elements that have higher spatial resolutions must
52 be compromised due to the lower spatial resolution of human elements like population (*Yang et
53 al., 2013*). Therefore, a comprehensive and sophisticated geographic research unit has not been
54 established, thus resulting in simulation results applicable only to macro planning and decision
55 making. Hence, the estimation of disaster exposure needs to incorporate greater spatial
56 heterogeneity and resolution.

57 Besides enhancement of the spatial scale, dynamic temporal simulation of disaster exposure has
58 gained increasing attention. Specifically, the dynamic evolution of disaster exposure at the macro
59 time scale considers exposure distribution as well as its variation during different development
60 periods (*Weis et al., 2016*). Therefore, this method is relatively mature and has led to abundant
61 research results. At the micro time scale, disaster-causing factors and disaster-bearing bodies
62 represented by populations are constantly varying. On the one hand, spatio-temporal changes in
63 disaster-causing factors (rainfall) result in corresponding dynamic changes in the characteristics
64 (water depth and velocity) of urban flood disasters. On the other hand, daily travel activities of
65 urban residents, such as commuting between residential and work or learning spaces, cause a
66 dynamic spatio-temporal distribution of the population. At the same time, the exposure to urban
67 flooding changes dramatically over a short period of time. To avoid or reduce disaster risks,
68 casualties, and property losses, different individuals are likely to adopt different adaptive behaviors,
69 such as delaying or cancelling travel plans, while the government is likely to adopt organizational



70 actions such as issuing warnings and evacuating residents (*Wan and Wang, 2017; Parker et al.,*
71 *1995*). Thus, the dynamic simulation of exposure requires the dynamic space-time simulation of
72 variations in the disaster, disaster-bearing bodies, as well as interactions between them. Modeling
73 of the temporal and spatial changes in natural disasters mainly uses the disaster system simulation
74 method, and the typical representative used is a hydrological or hydrodynamic model to simulate
75 flood disasters (*Werren et al., 2016*). The change simulation of the disaster-bearing body
76 (population) can use the method based on individual space-time mark data (*Liang et al., 2015*) and
77 the agent-based method (*Kang et al., 2012*). Although the former can acquire the human position
78 and moving track, it is difficult to identify the purpose of human activities, and human disaster
79 response behavior cannot be simulated. The agent-based model (ABM) can not only simulate the
80 population distribution but can also simulate the interaction among the population (as the disaster
81 victim), the hazard factors, and the disaster-pregnant environment (*Yin, et al., 2016b*). Current
82 research has used the ABM to simulate human responses to disasters, which, in turn, have been
83 used in natural disaster risk research (*Johnstone, 2012; Huang et al., 2015*). Nevertheless, the
84 simulation results do not reflect the exposure characteristics of the disaster-bearing bodies and
85 their dynamic changes (*Dawson et al., 2011*).

86 Therefore, the objectives of this study were to develop a novel method using the LISFLOOD-FP
87 model (Sect. 3.1) and an ABM (Sect. 3.2) to simulate the exposure of urban populations, roads,
88 and buildings to flooding under varying conditions and subsequently implement the method as a
89 pilot study in a real city. Several scenarios, including diverse flooding types and various responses
90 of residents to flooding, were considered in this regard. Additionally, dynamic features of the real
91 world were incorporated to improve the micro exposure analysis. This method was subsequently
92 applied to an urban area as a case study. Exposure simulation is a useful tool for estimation of



93 disaster vulnerability and assessment of losses, and the results of this study are likely to benefit
94 the relevant government agencies in assessing risk, issuing warnings, and planning emergency
95 responses to urban natural disasters.

96 **2. Study area and data source**

97 In this study, Lishui City in Zhejiang Province, China, was considered as the study region because
98 of the availability of the required data and flooding history. The urban district of Lishui is a largely
99 hilly and mountainous area, and the Oujiang River traverses its southern and eastern parts. The
100 study area is located in the central district of Lishui, covers an area of 43.4 km², and has a large
101 population of about 71673 (Fig. 1). The frequencies of heavy rainstorms and persistent
102 concentrated rainfall events rise sharply in May and June during the Meiyu flood period, which
103 often results in flood disasters. On August 20, 2014, a heavy rainfall event lasting a few days
104 produced a 50-year flood in Lishui and caused considerable loss of property.

105 The datasets used in this study included a digital elevation model and data for rivers, roads,
106 buildings, population, and observation data consisting of flow and water level. Traffic flow and
107 water accumulation data were used for validation. Table 1 describes the sources and uses of the
108 datasets.

109 **3. Methodology**

110 This study comprised three aspects: disaster simulation, human activity simulation, and dynamic
111 exposure assessment (Fig. 2). The first step included fluvial and pluvial flooding simulation based
112 on the LISFLOOD-FP model. The simulation of human activity utilized ABM to obtain the spatio-
113 temporal distribution of the population under different scenarios. Finally, the developed model



114 was combined with the results of the previous two steps to assess the dynamic exposure of the
 115 population, roads, and buildings to urban flooding.

116 **3.1 Flood models**

117 A wide variety of existing hydrological or hydrodynamic models are available that are capable of
 118 simulating fluvial or pluvial flooding, including the Storm Water Management Model (SWMM)
 119 (Rossman, 2015), LISFLOOD (Bates and De Roo, 2000), MIKE-SHE (DHI, 2000), MIKE-11
 120 (Havnø et al., 1995), MOUSE (Lindberg et al., 1989), HEC-RAS (Brunner, 2008), and HEC-HMS
 121 (Charley et al., 1995). LISFLOOD-FP (Bates et al., 2013) is a coupled 1D/2D hydraulic model
 122 based on a raster grid and was designed for research purposes at the University of Bristol.
 123 LISFLOOD-FP uses a square grid as the computational grid to simulate one-dimensional river
 124 hydraulic changes and two-dimensional floodplain hydraulic changes. The applicability of the
 125 model has been verified by several studies (Horritt and Bates, 2002; Bates and De Roo, 2000).
 126 Therefore, the LISFLOOD-FP model was chosen for the simulation of fluvial and pluvial flooding.

127 Floodplain flows were described in terms of the continuity and momentum equations discretized
 128 over a grid of square cells, which allowed the model to represent 2D dynamic flow fields for the
 129 floodplain. It assumed that the flow between two cells was simply a function of the free surface
 130 height difference between those cells:

$$131 \quad \frac{dh^{i,j}}{dt} = \frac{Q_x^{i-1,j} - Q_x^{i,j} + Q_y^{i,j-1} - Q_y^{i,j}}{\Delta x \Delta y}, \quad (1)$$

$$132 \quad Q_x^{i,j} = \frac{h_{flow}^{5/3}}{n} \left(\frac{h^{i-1,j} - h^{i,j}}{\Delta x} \right)^{1/2} \Delta y, \quad (2)$$



133 where $h^{i,j}$ is the free surface height of water at node (i,j) , Δx and Δy are the cell dimensions, n is
134 the effective grid scale Manning's friction coefficient for the floodplain, and Q_x and Q_y describe
135 the volumetric flow rates between the floodplain cells. Q_y is defined analogously to Q_x . The flow
136 depth, h_{flow} , represents the depth through which water can flow between two cells, and d is
137 defined as the difference between the highest free surface height of water in the two cells and the
138 highest bed elevation.

139 The types of flooding simulated in this study included pluvial and fluvial floods. Synthetic rainfall
140 data for a return period of 50 years used for pluvial flood simulation were simulated using the
141 Chicago hyetograph method (CHM) (Cen *et al.*, 1998). The rainfall data were determined using
142 the rainstorm intensity formula (Eq. (3)), rainfall duration time (T), and peak position (r).

$$143 \quad i = \frac{A(1+c \log P)}{167(t+b)^n}, \quad (3)$$

144 where i is the rainfall intensity (mm/min), P is the return period, and t is the time. A , b , c and n
145 are parameters related to the characteristics of the local rainstorm and need solutions. A is the
146 rainfall parameter, i.e. the design rainfall (mm) for 1 min at a 10 year return period, c is the rainfall
147 variation parameter (dimensionless), and b is the rainfall duration correction parameter, i.e. the
148 time constant (min) that can be added to convert the curve into a straight line after logarithmic
149 calculation of the two sides of the rainstorm intensity formula. n is the rainstorm attenuation index,
150 which is related to the return period. The rainfall duration was 6 hours (6 am to 12 pm), and the
151 accumulated rainfall was nearly 148 mm. Here, we fixed r at 0.2 based on the assumption that the
152 peak is located at the one fifth point of the design hyetograph. The parameters A , b , c and n were
153 estimated from the rainstorm intensity formula for Lishui City obtained from the "Zhejiang City
154 Rainstorm Intensity Formula Table" published by the Hangzhou Municipal Planning Bureau



155 (Table 2). The rainfall simulation results are shown in Fig. 3(a). The flow and water level input
156 data for fluvial flood simulation utilized observational data from Lishui's 50-year flood in 2014,
157 provided by the Liandu Hydrological Station (Fig. 3(b)). The flow data for the Daxi and Haoxi
158 rivers on August 20, 2014 were obtained from the Xiaobaiyan and Huangdu stations, respectively,
159 and the observational data for water levels at the outlets were those for the Kaitan Dam.

160 **3.2 ABM**

161 Several modeling techniques, often collectively referred to as social simulation, have been
162 successfully used to represent the behaviors of humans and organizations. These include event and
163 fault trees, Bayesian networks, microsimulation, cellular automata, system dynamics, and ABMs.
164 Research methods based on ABMs have been gradually introduced to the field of natural disaster
165 risk assessment. ABM is considered most suitable to address challenges associated with simulating
166 the complexity and dynamic variability of population exposure to flooding due to its capacity to
167 capture interactions and dynamic responses in a spatial environment.

168 An ABM is a computational method for simulating the actions and interactions of autonomous
169 decision-making entities in a network or a system to subsequently assess their effects on the system
170 as a whole. Individuals and organizations represent agents. Each agent individually assesses its
171 situation and makes decisions based on a set of rules. Agents may execute various behaviors
172 appropriate for the system component they represent—for example, producing or consuming.
173 Therefore, an ABM consists of a system of agents and the relationships between them. Even a
174 simple ABM can exhibit complex behavior patterns because a series of simple interactions
175 between individuals may result in more complex system-scale outcomes that could not have been
176 predicted just by aggregating individual agent behaviors.



177 The ABM was developed as a concept in the late 1940s, and substantial applications were realized
178 with the emergence of high-powered computing. Such applications include those in the political
179 sciences (*Axelrod, 1997*), management and organizational effectiveness, and the behavior of social
180 networks (*Sallach and Macal, 2001; Gilbert and Troitzsch, 2005*). In recent years, it has been
181 introduced to the geosciences and other fields to provide novel ideas for the study of modern
182 geography, including land use simulation and planning as well as residential choice and residential
183 space differentiation (*Benenson et al., 2002*). The urban flood disaster system is a typical complex
184 “natural and social” system. The introduction of ABM to simulate space-time distributions of
185 populations is expected to quantify the dynamic exposure of populations to urban flood disasters.
186 For example, *Dawson et al. (2011)* proposed a dynamic ABM for flood event management to
187 evaluate population vulnerability under different storm surge conditions, dam break scenarios,
188 flood warning times, and evacuation strategies.

189 **3.3 Spatio-temporal simulation of population distribution**

190 The individual travels were simulated using ABM by defining the activity patterns of different
191 types of residents to subsequently obtain the distribution of the population at each moment. The
192 ABM of residents’ travels established in this study included two core elements of agents and
193 activities, and two basic elements of blocks and networks. The travel survey data were used
194 according to the demographic properties of the agent to generate synthetic daily routines.

195 Residents were independent individuals with subjectivity. This study abstracted them as agents.
196 Only a limited number of agent classifications were used to reduce the number of agent types. The
197 types of agents were classified according to the social characteristics of the residents. Age and
198 gender characteristics mainly affect the ability of people to respond to disasters. The self-help



199 abilities of the minors under 18 years of age and residents older than 60 years are generally poor.
200 In the event of natural disasters, they are generally categorized as the objects of help. The middle-
201 aged group (18–60 years old) generally has greater physical strength with better ability to cope
202 with disasters. Unemployed people are more vulnerable to natural disasters. On the one hand, their
203 living environments and resistance to disasters are poor; on the other hand, their economic
204 conditions are limited, which impedes recovery after the disaster and seriously affects their daily
205 life in the short term. Education level is related to the possibility of receiving early warning
206 information by the individual. Individuals with higher education levels are more likely to respond
207 to early warning information and are more aware of disasters than others (*Terti et al., 2015; Shabou*
208 *et al., 2017*). Additionally, different travel modes have different effects on the activity patterns of
209 people as well as on exposure levels when disasters occur. Therefore, the agent types were divided
210 according to age, gender, employment status, education level, and travel mode.

211 Activities were classified as work, learning, leisure, recreation, shopping, rest, and travel. An
212 activity pattern consisted of a series of activities to describe the spatio-temporal distribution of the
213 agent. The location and scope of an agent were restricted to blocks and networks. Different types
214 of agents indicated different activity patterns, and the same agent type could also indicate different
215 activity patterns in different scenarios. To capture the variability in the travel survey and the
216 uncertainties in behavior, synthetic daily routines were described in probabilistic terms. Figure 4
217 presents an example of the synthetic daily routine of an agent with the following demographic
218 characteristics: female agent, aged 18–60 years, and unemployed. In this example, the agent started
219 the day at 8 am on a weekday. The agent then traveled by a school to drop the children off,
220 subsequently had a 0.8 probability of shopping, and so on.



221 The study area was discretized into several blocks to improve the spatial resolution of the exposure
222 results. The discretization procedure was conducted with geographic information system (GIS)
223 tools (*Lü et al., 2018*), and several factors, including rivers, roads, land use, and buildings, were
224 considered. Blocks were activity places for agents and represented the smallest unit of exposure.
225 This study divided the block into five categories: residential area, school, company, recreational
226 area, and others. Additionally, the residential areas were subdivided into I, II, III, and IV classes
227 according to the type of building.

228 In this study, the network referred to roads and restricted the spatial travel scope of an intelligent
229 agent. Rural roads, highways, and urban roads (including main roads, sub trunk roads, and its
230 branches) were included in the network. The route selection criteria were defined once the different
231 activities from each individual's schedule were located, and road section attributes were specified.
232 Although various factors are involved in the route choice process, several studies have indicated
233 that minimizing travel time is the principal criterion for selecting routes (*Papinski et al., 2009*;
234 *Ramming, 2001*; *Bekhor et al., 2006*). Therefore, the classical Dijkstra algorithm, a single-source
235 shortest path algorithm that provides trees of minimal total length and time in a connected set of
236 nodes, was selected in this study (*Dijkstra, 1959*). The activity pattern attributions concerned only
237 the starting times and durations of the activity sequences, thus indicating that the travel duration
238 for each individual was computed based on the distance between the different activity locations.
239 Therefore, the implemented schedules may be distorted compared to the assigned schedules in
240 terms of travel durations (*Terti et al., 2015*).

241 **3.4 Impacts of disasters on anthropogenic activities**



242 This study accounted for the adaptability or adjustment behavior of residents to disasters during
243 the disaster event. The type of activity and its sensitivity to disaster affected the residents' disaster
244 response behavior. Recreation and shopping activities were easier to cancel and postpone than
245 work and learning (*Cools et al., 2010*). The sensitivities of residents to disasters depended on their
246 socioeconomic characteristics and risk factors such as disaster- (flood-) related knowledge and
247 experience. People with higher education levels are more knowledgeable about disasters and are
248 more likely to receive early warning information and take effective measures (*Terti et al., 2015*).
249 Additionally, it is easier for workers to ignore the risks of a disaster (*Ruin et al., 2007; Drobot et*
250 *al., 2007*). Therefore, this study accounted for the impacts of education level on the response
251 behavior of residents to disaster events.

252 The impacts of a disaster on population distribution were determined by defining different activity
253 patterns and their changing probabilities. Figure 5 indicates activity patterns for unemployed adult
254 women during different disaster scenarios. The “bad weather” scenario was similar to the “daily
255 activity” pattern. For instance, the change in travel probability during “bad weather” due to a
256 rainstorm reflected the adaptive behavior of residents. The “warning” scenario assumed that the
257 government had issued early warning information at eight a.m., the schools had suspended classes
258 during the weekday, and the resident responses were stronger than those to the “bad weather”
259 scenario, thereby resulting in a greater difference in activity patterns.

260 **3.5 Dynamic exposure assessment**

261 The dynamic exposure was calculated based on the simulations of spatio-temporal distributions of
262 the population and flooding. Therefore, the exposure at each moment was calculated according to



263 the population distribution and flood data at that time. Based on the availability of data, this study
264 focused only on three types of disaster-bearing bodies, i.e., population, roads, and buildings.

265 (i) Population

266 Population exposure generally refers to the population exposed to the impacts of disaster events
267 and is characterized by regional population or population density. This study selected the exposed
268 population and accounted for vulnerable groups and road users. Among these, age was the primary
269 factor impacting the vulnerability. Specifically, the young (people under the age of 18 years) and
270 the elderly (people over 60 years old) were the vulnerable groups.

271 (ii) Roads

272 As the basic skeleton of a city, roads are not only the media for daily travel of passengers and
273 freight transportation but also disaster-bearing bodies (*Yin, et al., 2016a*), as they are vulnerable
274 to flood disasters. This study selected the number and lengths of exposed roads to reflect road
275 exposure.

276 (iii) Buildings

277 The aggravation of urban flooding has made building flooded more common in urban areas, thus
278 resulting in loss of internal property and construction structure. Additionally, the dynamic state of
279 building exposure is related to the safety of both the building as well as the nearby population. In
280 this study, the area of the exposed building and the depth of accumulated water in the building
281 were considered to be the building exposure.

282 **3.6 Scenario design**



283 The daily behaviors of people are characterized by certain patterns with regard to daily, weekly,
284 monthly, and annual cycles. The rainstorm (“bad weather”) and disaster response measures
285 adopted by the organization (“warning”) are likely to affect people’s daily behaviors. Therefore,
286 12 scenarios, representing different flooding types and human activities, were designed in this
287 study (Table 3). S1, S2, S7, and S8 were control groups that indicated human activity with no rain
288 and no warning, while the rest of the scenarios were experimental groups.

289 **4. Results**

290 **4.1 Model implementation and parameter setting**

291 As an important spatial data management and analysis technology, GIS plays an important role in
292 dynamic exposure analysis of urban floods. Because of the simplicity, readability and extensibility
293 of the Python programming language, an increasing number of research institutes are adopting it
294 for development. Therefore, the model was developed using the Visual Studio Code software
295 (*Visual studio code, 2018*) and Python programming language (*Python, 2018*). The development
296 of the graphical user interface (GUI), GIS module, and drawing module was realized by Qt (*Qt,*
297 *2018*), Geopandas (*Geopandas, 2018*), and Matplotlib (*Matplotlib, 2018*), respectively.

298 (i) Block generation

299 In this study, the study area was divided into 237 blocks based on the method introduced in Sect.
300 3.3. The block types and their spatial distributions are shown in Fig. 6 and Fig. 7, respectively.
301 Most of the blocks in the study area were categorized as residential area, while blocks of
302 recreational areas and others (which indicated rivers) were few and concentrated.

303 (ii) Parameter setting



304 Since the census did not identify individuals according to addresses, at the start of each simulation,
305 an agent population with the same distributions of age, gender, employment, education level, and
306 travel mode was randomly located within the residential area for the case study. The synthetic
307 daily routines were described in probabilistic terms to capture the variability in the travel survey
308 and uncertainties in behavior.

309 Additionally, to reduce the number of agent types, only a limited number of agent classifications
310 were used. The distribution of population characteristics for Liandu District is shown in Table 4.
311 The agents were divided into 18 types for daily (non-disaster) scenarios and 24 types for disaster
312 scenarios based on the influence of education level on the individual disaster response behavior
313 (Fig. 8).

314 (iii) Exposure threshold

315 Although flood fatalities can occur through a number of mechanisms, such as physical trauma,
316 heart attack, or electrocution, drowning accounts for two-thirds of the fatalities (*Jonkman and*
317 *Kelman, 2005*). Previous research has established that the probability of death or serious injury as
318 a result of exposure to flooding (*Abt et al., 1989; Karvonen et al., 2000; Lind et al., 2004; Jonkman*
319 *and Penning - Rowsell, 2008*) is dominated by (1) the depth of floodwater and (2) the velocity of
320 floodwater. Additionally, the rate of water level rise can also play an important role in this regard.
321 However, other factors, such as age, fitness level, height, and weight of the individual, are also
322 important for determining their vulnerability to disasters. A comprehensive review of the flood-
323 related casualty data and methods to assess the risk of death or serious harm to people caused by
324 flooding is provided by the *Department for Environment Food and Rural Affairs and Environment*
325 *Agency (2003)* and *Jonkman and Penning - Rowsell (2008)*. In this study, rather than predicting



326 mortality (which is subject to random factors as well as those mentioned previously), exposure to
327 floodwater depths of 25 cm or greater under relatively fast flowing (2.5 m/s or greater) conditions
328 was established as the threshold for most vulnerable people (*DEFRA and Environment Agency,*
329 *2003*). This provided a conservative estimate of individuals vulnerable to floodwater rather than
330 an estimate of mortality (*Dawson et al., 2011*).

331 Since building steps (thresholds) exert a blocking effect on shallow flooding, they are likely to
332 reduce the degree of flooding by restricting the flood water to the outside of the building, thereby
333 reducing the exposure of the building. Therefore, this study assigned building step heights to
334 corresponding block types according to the architectural design standards of China and the actual
335 conditions of the study area (Table 5). It should be noted that the block type “Other” constituted
336 rivers and did not contain buildings. Therefore, the exposure of the building was determined
337 according to the depth of the flood and the height of the building steps. The depth of the water
338 entering the building was the difference between the depth of the flood and the height of the step.

339 **4.2 Flood simulation**

340 Figure 9 indicates the accumulated water depths and velocities of pluvial and fluvial floods in the
341 study area. As is evident, the pluvial and fluvial floods exerted significant impacts, and the urban
342 area near the Oujiang River was the most severely flooded area. Additionally, water is also
343 accumulated in the inner areas of the city, mainly on roads, in case of pluvial flood disasters. The
344 variations in water depths and velocities for eight severely flooded areas (including blocks and
345 roads) are presented in Fig. 10. As indicated, evident spatio-temporal variations in flooding were
346 observed. Figures 9 and 10 indicate that water depth was the main factor causing life and property
347 losses, whereas water velocity had little or no effect.



348 **4.3 Simulation of the spatio-temporal distribution of population**

349 The population spatio-temporal distribution was simulated based on six scenarios: (1) daily,
350 weekday (S1, S7); (2) daily, weekend (S2, S8); (3) bad weather, weekday (S3, S9); (4) bad weather,
351 weekend (S4, S10); (5) warning, weekday (S5, S11); (6) warning, weekend (S6, S12). Figure 10
352 indicates the population variation for blocks and roads for the six scenarios. Figure 11(a) indicates
353 that, among the three weekend scenarios, the population in the playground (Block 77) changed
354 more than the population in the company (Block 113). Figure 11(b) indicates that the population
355 on the roads was volatile, and the morning peak hour during the weekend was delayed by an hour
356 in comparison to that during the weekdays. The population distribution in the study area is shown
357 in Fig. 12. The population was unevenly distributed and concentrated in recreational and
358 residential areas over the weekend. However, the population distribution on weekdays was
359 relatively uniform. The concurrent population distribution for the six scenarios changed
360 significantly during the weekend, while the distribution for weekdays changed little.

361 Figures 11 and 12 indicate that the population change patterns were different for different blocks
362 types. The daily routines of several people started from the residential area (home) in the morning,
363 followed by school or company blocks during weekdays and recreational areas during weekends,
364 and, finally, concluded with a return to the residential area at night. During the occurrence of
365 rainstorms or the reception of warning messages, different types of people reacted differently
366 (continuing, postponing, or cancelling the originally planned activities). Vulnerable people, like
367 the elderly and children, and sensitive people (such as the homeless) were more likely to cancel
368 travel plans. Additionally, recreational activities were more likely to be cancelled than were
369 learning and work activities.



370 **4.4 Exposure assessment**

371 Figure 13 presents the population exposure variation for two selected areas. The difference
372 between pluvial and fluvial flood scenarios could be attributed to differences in the changes and
373 degrees of water accumulation. Figure 13(a) indicates that population exposure was the highest for
374 the daily scenario, followed by the bad weather scenario and minimum warning scenario. However,
375 as indicated in Fig. 13(b), the population was most exposed to both weekend and weekday warning
376 scenarios. This is attributed to the assumption that the disaster response behavior adopted by
377 residents was to reduce travel, i.e., the refuge of residents was the residential area. Additionally,
378 the response was not based on the exposure of the residential area. Therefore, when residential
379 areas, such as Block 6, were exposed to floods, the residents chose to reduce travel, thus resulting
380 in an increase in the population of residential areas and consequently increasing the population
381 exposure. According to the analysis of the 12 scenarios, the government departments can carry out
382 disaster prevention and mitigation measures for areas with large amounts of population exposure,
383 such as evacuation prior to the disaster, and initiate key rescue operations during the disaster. The
384 method proposed in this study can also help determine vulnerable populations and road users in
385 the exposed blocks. Because we had considered vulnerable people and road users when we
386 constructed the population groups (agents), we can get similar information from the results of
387 vulnerable populations and road users in the exposed blocks, like the exposed population. Such
388 information is of great practical significance.

389 Figure 14 presents variations in the road and building exposures of two selected areas with serious
390 flooding. The road and building exposures for the study area are presented in Fig. 15. It can be
391 concluded that road and building exposures during pluvial and fluvial floods also varied with the
392 flood depth. Additionally, the exposed road length of the block was fluctuant, while the building



393 was either entirely exposed or not exposed. Furthermore, the area of the road affected by pluvial
394 and fluvial floods was greater than that of the buildings. As indicated in Fig. 15, exposed buildings
395 were present only in a few areas (blocks), while roads were affected in several areas. Additionally,
396 buildings were least exposed due to high thresholds or the number of building steps designed and
397 built in recent years, while roads and population were severely affected by floods.

398 **4.5 Validation**

399 The flooded urban roads and locations in Lishui during the 50-year flood in 2014 were as follows:
400 the city had 10 flooded roads and 18 water accumulation points. The actual hydrological points
401 were selected and combined with the urban flooding results simulated by the prototype system.
402 The water accumulation distribution is indicated in Fig. 16.

403 To avoid overlapping with the simulated water accumulation results for roads, the actual flooding
404 points in the figure only included road junctions and the entirety of Gucheng road (the Lutang
405 Street to Dayou Street section), and Liyang Street (which connected the senior middle school to
406 the Sanyan temple section) was represented by corresponding intersection points. Figure 16
407 indicates that both the simulation results and the actual water accumulation points were mainly
408 distributed along the river. The simulated water accumulation area (Fig. 16(a)) included roads in
409 the center of the city and was larger than the actual flooding area. This difference could be
410 attributed to different definitions of “water accumulation”. The simulation results presented in
411 Figure 16 included all areas where the accumulated water depth during the flooding period was
412 greater than 15 cm. The actual water accumulation point was defined as one experiencing rainfall
413 greater than 50 mm over a 24 hour period. Additionally, it was characterized by the water
414 accumulation depth of the road reaching 15 cm (the meteorological department issued the blue



415 rainstorm warning at this level), the water withdrawal time reaching one hour, and the water
416 accumulation scope value being greater than 50 m². Certain gaps existed between the observational
417 data and the actual flow since the observation station was far from the study area. Hence, the results
418 indicated that the simulated water accumulation area during the fluvial flood (Fig. 16 (b)) was
419 smaller than that of the actual situation.

420 The reliability of the simulation of the spatio-temporal population distribution was indirectly
421 verified by utilizing the traffic flow data from June 24 to July 7, 2017. The morning and evening
422 peak hours on weekdays and weekends, the simulated total number of residents passing the four
423 intersections (such as the junction of the Liqing and Huayuan roads) during peak hours, and the
424 actual measured traffic flow at the intersections are shown in Fig. 17. The traffic flow data in Fig.
425 17 are multi-day average results.

426 In theory, the simulated value should be much larger than the measured value since the former
427 indicates the number of people while the latter represents the number of cars and buses. However,
428 as indicated in Fig. 17, the simulated value was close to the measured value. This could be
429 attributed to the assumption that the study area was closed and the simulated population was the
430 number of permanent residents, excluding the migrant population. In reality, the number of
431 migrants in the urban area during daytime is large owing to its geographical location. Moreover,
432 this study simplified human activities when simulating the spatio-temporal distribution of the
433 population. Therefore, the number of pedestrians on the road was small. However, both the
434 simulated and measured values were essentially similar with regard to changes in their trends.
435 Therefore, the simulation method for the spatio-temporal distribution of population is feasible, and
436 the results are reliable.



437 **5. Conclusions**

438 Urban flooding considerably impacts the daily lives of residents and not only affects commuting
439 but also causes casualties and traffic congestion. This study proposed a method for obtaining high-
440 resolution dynamic exposure to urban flooding. First, the spatio-temporal distributions of pluvial
441 and fluvial floods were simulated by the LISFLOOD-FP model. Second, the responses of residents
442 to bad weather and government measures (warnings) were incorporated to develop an ABM to
443 simulate residents' activities during flooding. Finally, urban exposure during different flood
444 scenarios was comprehensively simulated and was based on the population and hydrological
445 simulation results, road and building data, and the case study of the Lishui urban district.

446 The method developed could predict floods as well as the exposure of buildings, roads, and the
447 population at different times and locations. Additionally, it could provide effective reference
448 information for residents' travels and urban disaster management. In summary, this study had four
449 main elements. First, different spatio-temporal distributions of water depth and velocity
450 predictions were obtained using the LISFLOOD-FP model. Second, an ABM was utilized to
451 simulate the spatio-temporal distributions of the population. Third, the impacts of pluvial and
452 fluvial floods on buildings were found to be small, while that on roads and the population was
453 evident. Finally, if residents simply reduced their travels (stayed at home), the exposure of the
454 population in the exposed residential areas increased.

455 It should be noted that there is no comprehensive way to verify the proposed method. This is
456 because parameters of human behavior and psychological processes are difficult (or, to some
457 extent, impossible) to obtain. In this study, the proposed method was verified indirectly. The actual
458 traffic information for each road intersection was collected and compared with the simulated
459 population results. Additionally, the information for actual water accumulation points was



460 compared with the simulated water accumulation results. However, a few limitations persist. For
461 instance, considerable uncertainties regarding the use and design of the ABM exist. These include
462 differences in the responses of residents of the same type to disasters in the same scenario.
463 Therefore, this study simply attempted to reflect reality. Moreover, simplification of the behavior
464 patterns and disaster responses of residents is inevitable, thus resulting in differences between the
465 simulation results and reality. In addition, the investigation of different durations and intensities
466 of the rainstorm is also relevant. However, the inclusion of other factors was beyond the scope of
467 this research. Therefore, future studies should focus on optimizing the proposed method and
468 incorporating the effects of different durations and intensities of rainstorms.

469 **Acknowledgements**

470 This study is supported by the National Natural Science Foundation of China (Nos: 41771424,
471 41871299) and National Key R & D Program of China (Nos: 2018YFB0505500,
472 2018YFB0505502). Dawei Han and Lu Zhuo are supported by Newton Fund via Natural
473 Environment Research Council (NERC) and Economic and Social Research Council (ESRC)
474 (NE/N012143/1).

475 **References**

- 476 Abt, S. , Wittier, R. , Taylor, A. and Love, D.: HUMAN STABILITY IN A HIGH FLOOD
477 HAZARD ZONE1. JAWRA Journal of the American Water Resources Association, 25:
478 881-890, <https://doi.org/10.1111/j.1752-1688.1989.tb05404.x>, 1989.
- 479 Atta-Ur-Rahman, D.: Disaster risk management, 2014.
- 480 Axelrod, R.: The complexity of cooperation: Agent-based models of competition and
481 collaboration (Vol. 3). Princeton University Press, 1997.
- 482 Bates, P. D., and De Roo, A. P. J.: A simple raster-based model for flood inundation simulation.
483 Journal of hydrology, 236(1-2), 54-77, [https://doi.org/10.1016/S0022-1694\(00\)00278-X](https://doi.org/10.1016/S0022-1694(00)00278-X),
484 2000.



- 485 Bates, P., Trigg, M., Neal, J., Dabrowa, A.: LISFLOOD-FP User manual, Code release 5.9.6,
486 School of Geographical Sciences, University of Bristol, University Road, Bristol, BS8 1SS,
487 UK, 2013. Available online at University of [https://www.bristol.ac.uk/media-](https://www.bristol.ac.uk/media-library/sites/geography/migrated/documents/lisflood-manual-v5.9.6.pdf)
488 [library/sites/geography/migrated/documents/lisflood-manual-v5.9.6.pdf](https://www.bristol.ac.uk/media-library/sites/geography/migrated/documents/lisflood-manual-v5.9.6.pdf).
- 489 Bekhor, S., Ben-Akiva, M. E., and Ramming, M. S.: Evaluation of choice set generation
490 algorithms for route choice models. *Annals of Operations Research*, 144(1), 235-247,
491 <https://doi.org/10.1007/s10479-006-0009-8>, 2006.
- 492 Benenson, I., Omer, I., and Hatna, E.: Entity-based modeling of urban residential dynamics: the
493 case of Yaffo, Tel Aviv. *Environment and Planning B: Planning and Design*, 29(4), 491-
494 512, <https://doi.org/10.1068/b1287>, 2002.
- 495 Brunner, G. W.: HEC-RAS River Analysis System User's Manual Version 4.0. US Army Corps
496 of Engineers, Hydrologic Engineering Center. Report CPD-68, 2008.
- 497 Cen, G., Shen, J., and Fan, R.: Research on rainfall pattern of urban design storm. *Advances in*
498 *Water Science*, 9(1), 41-46, <https://doi.org/10.14042/j.cnki.32.1309.1998.01.007>, 1998.
- 499 Charley, W., Pabst, A., Peters, J.: The Hydrologic Modeling System (HEC-HMS): Design and
500 Development Issues. Hydrological Engineering Center, US Army Corps of Engineers,
501 Technical Paper No. 149, 1995.
- 502 Chen, Y., Zhou, H., Zhang, H., Du, G., and Zhou, J.: Urban flood risk warning under rapid
503 urbanization. *Environmental research*, 139, 3-10,
504 <https://doi.org/10.1016/j.envres.2015.02.028>, 2015.
- 505 Cools, M., Moons, E., Creemers, L., and Wets, G.: Changes in travel behavior in response to
506 weather conditions: do type of weather and trip purpose matter?. *Transportation Research*
507 *Record: Journal of the Transportation Research Board*, (2157), 22-28,
508 <https://doi.org/10.3141/2157-03>, 2010.
- 509 Danish Hydraulic Institute (DHI): MIKE SHE Water movement user manual. DHI Water &
510 Environment, 2000.
- 511 Dankers, R., and Feyen, L.: Climate change impact on flood hazard in Europe: An assessment
512 based on high - resolution climate simulations. *Journal of Geophysical Research:*
513 *Atmospheres*, 113(D19), <https://doi.org/10.1029/2007JD009719>, 2008.
- 514 Dawson, R. J., Peppe, R., and Wang, M.: An agent-based model for risk-based flood incident
515 management. *Natural hazards*, 59(1), 167-189, <https://doi.org/10.1007/s11069-011-9745-4>,
516 2011.
- 517 DEFRA and Environment Agency.: Flood risks to people phase 1: R&D Technical Report
518 FD2317. DEFRA, London, 2003.
- 519 Dijkstra, E. W.: A note on two problems in connexion with graphs. *Numerische mathematik*,
520 1(1), 269-271, 1959.
- 521 Drobot, S. D., Benight, C., and Grunfest, E. C.: Risk factors for driving into flooded roads.
522 *Environmental Hazards*, 7(3), 227-234, <https://doi.org/10.1016/j.envhaz.2007.07.003>, 2007.



- 523 Gain, A. K., Mojtahed, V., Biscaro, C., Balbi, S., and Giupponi, C.: An integrated approach of
524 flood risk assessment in the eastern part of Dhaka City. *Natural Hazards*, 79(3), 1499-1530,
525 <https://doi.org/10.1007/s11069-015-1911-7>, 2015.
- 526 Geopandas: <http://geopandas.org/>, 2018.
- 527 Gilbert, N., and Troitzsch, K.: *Simulation for the social scientist*. McGraw-Hill Education (UK),
528 2005.
- 529 Guo, E., Zhang, J., Ren, X., Zhang, Q., and Sun, Z.: Integrated risk assessment of flood disaster
530 based on improved set pair analysis and the variable fuzzy set theory in central Liaoning
531 Province, China. *Natural hazards*, 74(2), 947-965, [https://doi.org/10.1007/s11069-014-](https://doi.org/10.1007/s11069-014-1238-9)
532 1238-9, 2014.
- 533 Hammond, M. J., Chen, A. S., Djordjević, S., Butler, D., and Mark, O.: Urban flood impact
534 assessment: A state-of-the-art review. *Urban Water Journal*, 12(1), 14-29,
535 <https://doi.org/10.1080/1573062X.2013.857421>, 2015.
- 536 Havnø, K., Madsen, M. N., and Dørgje, J.: MIKE 11—a generalized river modelling package.
537 *Computer models of watershed hydrology*, 733-782, 1995.
- 538 Horritt, M. S., and Bates, P. D.: Evaluation of 1D and 2D numerical models for predicting river
539 flood inundation. *Journal of hydrology*, 268(1-4), 87-99, [https://doi.org/10.1016/S0022-](https://doi.org/10.1016/S0022-1694(02)00121-X)
540 1694(02)00121-X, 2002.
- 541 Huang, H., Fan, Y., Yang, S., Li, W., Guo, X., Lai W., and Wang H.: A multi-agent based
542 theoretical model for dynamic flood disaster risk assessment. *Geographical Research*,
543 <https://doi.org/10.1875-1886.10.11821/dlyj20151006>, 2015.
- 544 IPCC.: Summary for Policymakers. In: *Managing the Risks of Extreme Events and Disasters to*
545 *Advance Climate Change Adaptation. A Special Report of Working Groups I and II of the*
546 *Intergovernmental Panel on Climate Change*. Cambridge University Press, Cambridge, UK,
547 and New York, NY, USA, pp. 3-21, 2012.
- 548 Johnstone, M. A.: Life safety modelling framework and performance measures to assess
549 community protection systems: application to tsunami emergency preparedness and dam
550 safety management, Ph.D. thesis, University of British Columbia, 2012.
- 551 Jonkman, S. N., and Kelman, I.: An analysis of the causes and circumstances of flood disaster
552 deaths. *Disasters*, 29(1), 75-97, <https://doi.org/10.1111/j.0361-3666.2005.00275.x>, 2005.
- 553 Jonkman, S. N., and Penning - Rowsell, E.: Human Instability in Flood Flows 1. *JAWRA*
554 *Journal of the American Water Resources Association*, 44(5), 1208-1218,
555 <https://doi.org/10.1111/j.1752-1688.2008.00217.x>, 2008.
- 556 Kang, T., Zhang, X., Zhao, Y., Wang, Y., and Zhang, W.: Agent-based Urban Population
557 Distribution Model. *Scientia Geographica Sinica*, 32(7): 90-797,
558 <https://doi.org/10.13249/j.cnki.sgs.2012.07.003>, 2012.
- 559 Karvonen, R. A., Hepojoki, A., Huhta, H. K., and Louhio, A.: The use of physical models in
560 dam-break analysis. *RESCDAM Final Report*. Helsinki University of Technology, Helsinki,
561 Finland, 2000.



- 562 Liang, Y., Wen, J., Du, S., Xu, H., and Yan J.: Spatial-temporal Distribution Modeling of
563 Population and its Applications in Disaster and Risk Management. *Journal of*
564 *Catastrophology*, 30(04):220-228, <https://doi.org/10.3969/j.issn.1000-811X.2015.04.038>,
565 2015.
- 566 Lind, N., Hartford, D., and Assaf, H.: Hydrodynamic models of human stability in a flood 1.
567 *JAWRA Journal of the American Water Resources Association*, 40(1), 89-96,
568 <https://doi.org/10.1111/j.1752-1688.2004.tb01012.x>, 2004.
- 569 Lindberg, S., Nielsen, J. B., and Carr, R.: An integrated PC-modelling system for hydraulic
570 analysis of drainage systems. In *Watercomp'89: The First Australasian Conference on*
571 *Technical Computing in the Water Industry; Preprints of Papers (p. 127)*. Institution of
572 Engineers, Australia, 1989.
- 573 Lü, G., Batty, M., Strobl, J., Lin, H., Zhu, A. X., and Chen, M.: Reflections and speculations on
574 the progress in Geographic Information Systems (GIS): a geographic perspective.
575 *International Journal of Geographical Information Science*, 1-22,
576 <https://doi.org/10.1080/13658816.2018.1533136>, 2018.
- 577 Mahe, G., Paturel, J. E., Servat, E., Conway, D., and Dezetter, A.: The impact of land use change
578 on soil water holding capacity and river flow modelling in the Nakambe River, Burkina-
579 Faso. *Journal of Hydrology*, 300(1-4), 33-43, <https://doi.org/10.1016/j.jhydrol.2004.04.028>,
580 2005.
- 581 Mansur, A. V., Brondízio, E. S., Roy, S., Hetrick, S., Vogt, N. D., and Newton, A.: An
582 assessment of urban vulnerability in the Amazon Delta and Estuary: a multi-criterion index
583 of flood exposure, socio-economic conditions and infrastructure. *Sustainability Science*,
584 11(4), 625-643, <https://doi.org/10.1007/s11625-016-0355-7>, 2016.
- 585 Matplotlib: <https://matplotlib.org/>, 2018.
- 586 Moel, H. D., Aerts, J. C., and Koomen, E.: Development of flood exposure in the Netherlands
587 during the 20th and 21st century. *Global Environmental Change*, 21(2), 620-627,
588 <https://doi.org/10.1016/j.gloenvcha.2010.12.005>, 2011.
- 589 Papinski, D., Scott, D. M., and Doherty, S. T.: Exploring the route choice decision-making
590 process: A comparison of planned and observed routes obtained using person-based GPS.
591 *Transportation research part F: traffic psychology and behaviour*, 12(4), 347-358,
592 <https://doi.org/10.1016/j.trf.2009.04.001>, 2009.
- 593 Parker, D., Fordham, M., Tunstall, S., and Ketteridge, A. M.: Flood warning systems under stress
594 in the United Kingdom. *Disaster Prevention and Management: An International Journal*,
595 4(3), 32-42, <https://doi.org/10.1108/09653569510088050>, 1995.
- 596 Python: <https://www.python.org/>, 2018.
- 597 Qt: <https://www.qt.io/>, 2018.
- 598 Ramming, M. S.: Network knowledge and route choice, Unpublished Ph. D. Thesis,
599 Massachusetts Institute of Technology, 2001.
- 600 Rossman, L. A.: Storm water management model user's manual Version 5.1 EPA-600/R-
601 14/413b[z]. National Risk Management Laboratory Laboratory Office of Research and



- 602 Development U. S. Environmental Protection Agency, 2015. Available online at
603 <https://nepis.epa.gov/Exe/ZyPDF.cgi/P100N3J6.PDF?Dockey=P100N3J6.PDF>
- 604 Röthlisberger, V., Zischg, A. P., and Keiler, M.: Identifying spatial clusters of flood exposure to
605 support decision making in risk management. *Science of the total environment*, 598, 593-
606 603, <https://doi.org/10.1016/j.scitotenv.2017.03.216>, 2017.
- 607 Ruin, I., Gaillard, J. C., and Lutoff, C.: How to get there? Assessing motorists' flash flood risk
608 perception on daily itineraries. *Environmental hazards*, 7(3), 235-244,
609 <https://doi.org/10.1016/j.envhaz.2007.07.005>, 2007.
- 610 Sallach, D. L., and Macal, C. M.: Introduction: The simulation of social agents. *Social Science*
611 *Computer Review*, 19(3), 245-248, <https://doi.org/10.1177/089443930101900301>, 2001.
- 612 Shabou, S., Ruin, I., Lutoff, C., Debionne, S., Anquetin, S., Creutin, J. D., and Beaufils, X.:
613 MobRISK: a model for assessing the exposure of road users to flash flood events. *Natural*
614 *Hazards and Earth System Sciences*, 17(9), 1631, [https://doi.org/10.5194/nhess-17-1631-](https://doi.org/10.5194/nhess-17-1631-2017)
615 2017, 2017.
- 616 Shi, P.: Theory and practice of disaster study. *Journal of Natural Disasters*, 4, 8-19, 1996.
- 617 Terti, G., Ruin, I., Anquetin, S., and Gourley, J. J.: Dynamic vulnerability factors for impact-
618 based flash flood prediction. *Natural Hazards*, 79(3), 1481-1497.
619 <https://doi.org/10.1007/s11069-015-1910-8>, 2015.
- 620 Visual studio code: <https://code.visualstudio.com/>, 2018.
- 621 Wan, H., Wang, J.: Analysis of Public Adaptive Behaviors to Drought and Flood Disasters in
622 Middle Reaches of Weihe River:A Case Study on Qishan County of Shaanxi Province. *Acta*
623 *Agriculturae Jiangxi*, <https://doi.org/10.19386/j.cnki.jxnyxb.2017.05.21>, 2017.
- 624 Weis, S. W. M., Agostini, V. N., Roth, L. M., Gilmer, B., Schill, S. R., Knowles, J. E., and
625 Blyther, R.: Assessing vulnerability: an integrated approach for mapping adaptive capacity,
626 sensitivity, and exposure. *Climatic Change*, 136(3-4), 615-629,
627 <https://doi.org/10.1007/s10584-016-1642-0>, 2016.
- 628 Werren, G., Reynard, E., Lane, S. N., and Balin, D.: Flood hazard assessment and mapping in
629 semi-arid piedmont areas: a case study in Beni Mellal, Morocco. *Natural Hazards*, 81(1),
630 481-511, <https://doi.org/10.1007/s11069-015-2092-0>, 2016.
- 631 Yang, X., Yue, W., and Gao, D.: Spatial improvement of human population distribution based on
632 multi-sensor remote-sensing data: an input for exposure assessment. *International journal of*
633 *remote sensing*, 34(15), 5569-5583, <https://doi.org/10.1080/01431161.2013.792970>, 2013.
- 634 Yin, Z.: Research of urban natural disaster risk assessment and case study, Ph.D. thesis, East
635 china normal university, Shanghai, China, 2009.
- 636 Yin, J., Yu, D., and Wilby, R.: Modelling the impact of land subsidence on urban pluvial
637 flooding: A case study of downtown Shanghai, China. *Science of the Total Environment*,
638 544, 744-753, <https://doi.org/10.1016/j.scitotenv.2015.11.159>, 2016a.
- 639 Yin, W., Yu, H., Cui, S., and Wang, J.: Review on methods for estimating the loss of life
640 induced by heavy rain and floods. *Progress in Geography*, 35(2), 148-158,
641 <https://doi.org/10.18306/dlkxjz.2016.02.002>, 2016b.



642 **Figure 1.** Location of the study area (left) and a digital elevation model indicating the specific
643 details of the study area (right).

644 **Figure 2.** Overview of the dynamic exposure simulation to urban flooding.

645 **Figure 3.** Rainfall simulation results based on the CHM method, and observational data used for
646 fluvial flood simulation.

647 **Figure 4.** A synthetic daily routine generated from the travel survey and census data for an
648 unemployed female agent aged 18–60 years.

649 **Figure 5.** Activity patterns for an unemployed female agent aged 18–60 years during disaster
650 scenarios. (a) Bad weather (weekday) (b) Warning (weekday) (c) Bad weather (weekend) (d)
651 Warning (weekend).

652 **Figure 6.** Number of different block types.

653 **Figure 7.** Spatial distribution of blocks.

654 **Figure 8.** Agent types for daily and disaster scenarios.

655 **Figure 9.** Accumulated water depths and velocities. T means time here.

656 **Figure 10.** Changes in the surface water depths and velocities for eight severely flooded areas.
657 The “dep” indicates water depth, and “vel” indicates water velocity.

658 **Figure 11.** Population changes in blocks and roads for the six scenarios.

659 **Figure 12.** Population distribution for the six scenarios. T means time here.

660 **Figure 13.** Changes in the population exposure of two blocks for the 12 scenarios. Block 168 was
661 a recreational area, and Block 6 was a residential area.

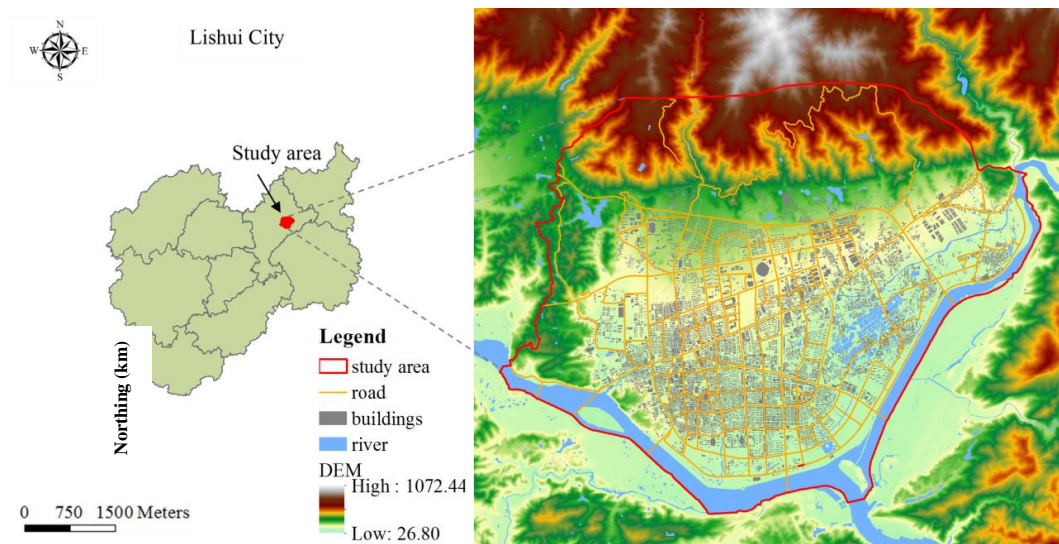
662 **Figure 14.** Changes in road and building exposures in severely flooded blocks. The exposed road
663 length and building area represent road and building exposures, respectively.

664 **Figure 15.** Map of road and building exposures. T means time here.



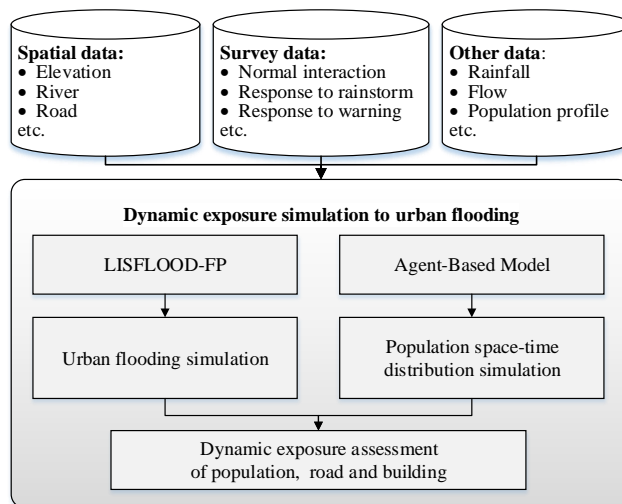
665 **Figure 16.** Map of the flooded area indicating the flooding simulation and the real flood in 2014.
666 The information for the flooded area was provided by Lishui City Housing and Urban-Rural
667 Construction Bureau.

668 **Figure 17.** Traffic flow and population simulation results during peak hours on weekdays and
669 weekends. The traffic flow data were provided by the Lishui City Traffic Bureau. Real means
670 measured value here. LQ is Liqing Road, KF is Kaifa Road, HY is Huayuan Road, ZJ is Zijin
671 Road, and LT is Lutang Street.



672

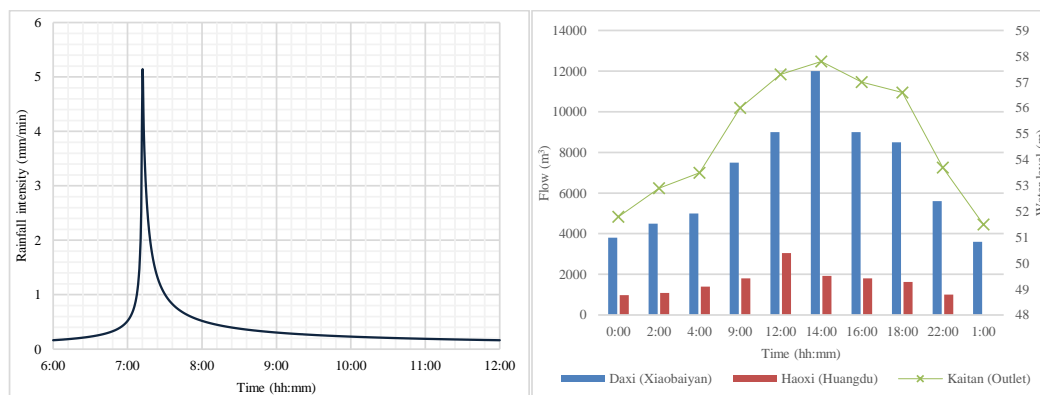
673 **Figure 1.** Location of the study area (left) and a digital elevation model indicating the specific
674 details of the study area (right).



675

676 **Figure 2.** Overview of the dynamic exposure simulation to urban flooding.

677



678

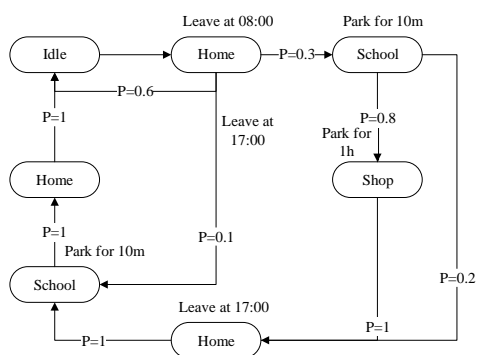
679 (a) Rainfall simulation data

(b) Observational data

680 **Figure 3.** Rainfall simulation results based on the CHM method, and observational data used for
681 fluvial flood simulation.

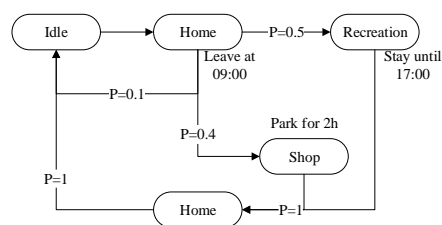


682



683

(a) Activity on weekdays



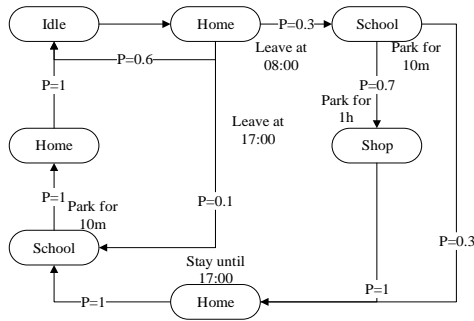
(b) Activity on weekends

684 **Figure 4.** A synthetic daily routine generated from the travel survey and census data for an
 685 unemployed female agent aged 18–60 years.

686

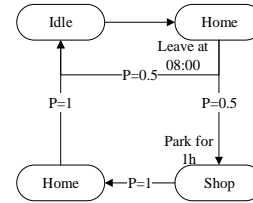


687



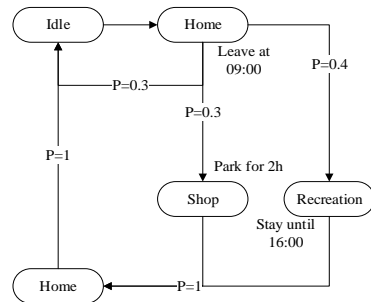
688

(a) Bad weather (weekday)



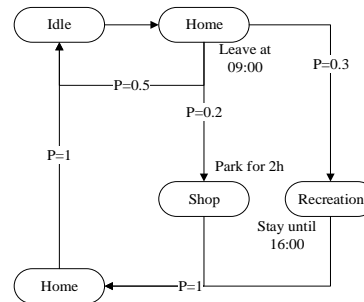
(b) Warning (weekday)

689



690

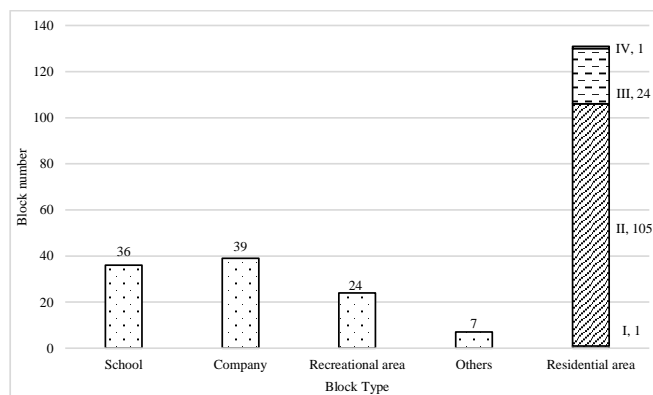
(c) Bad weather (weekend)



(d) Warning (weekend)

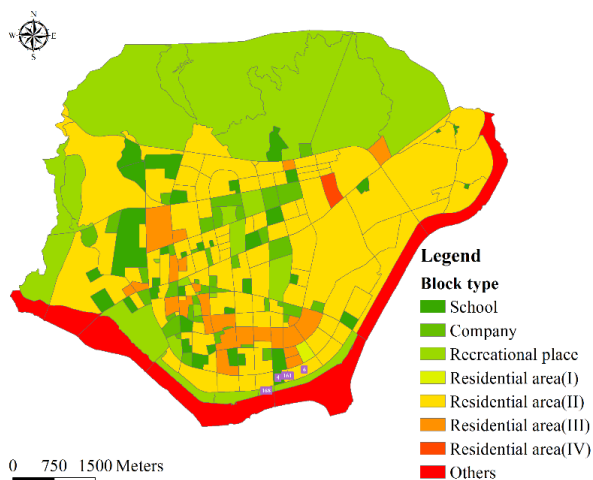
691 **Figure 5.** Activity patterns for an unemployed female agent aged 18–60 years during disaster
 692 scenarios. (a) Bad weather (weekday) (b) Warning (weekday) (c) Bad weather (weekend) (d)
 693 Warning (weekend).

694



695

696 **Figure 6.** Number of different block types.



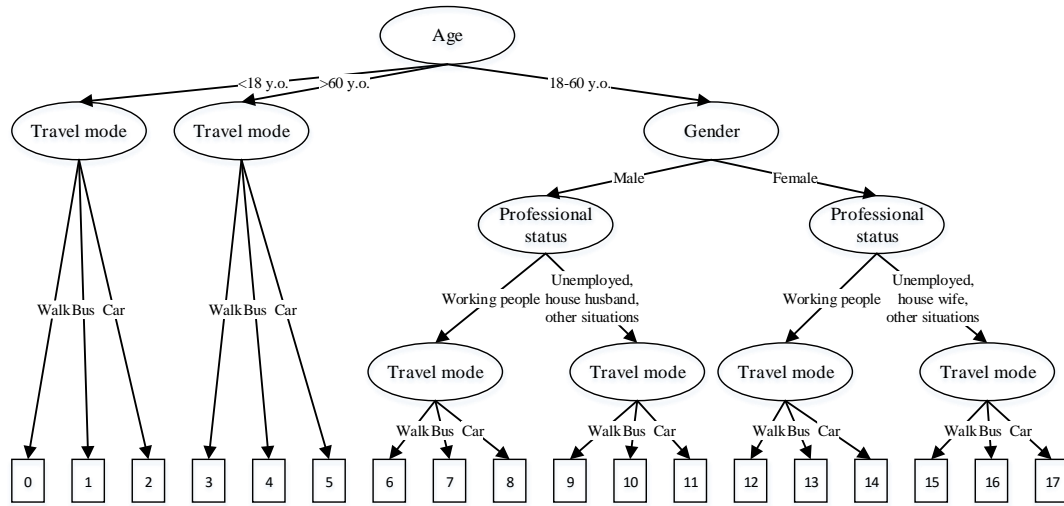
697

698 **Figure 7.** Spatial distribution of blocks.

699

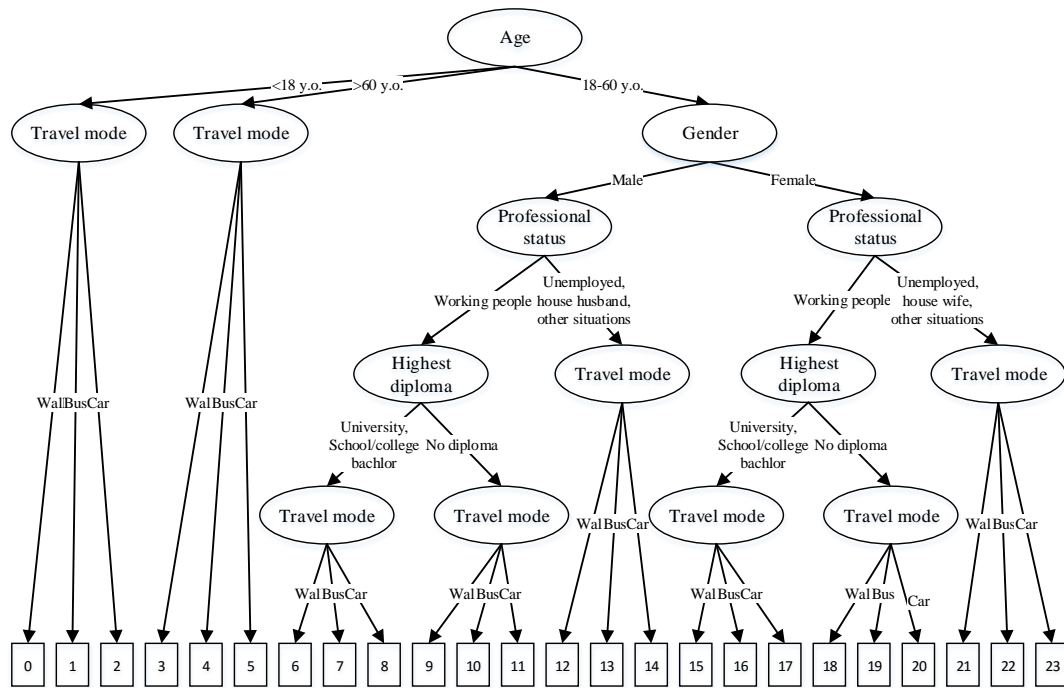


700
 701



(a) Agent types for daily scenarios

702
 703

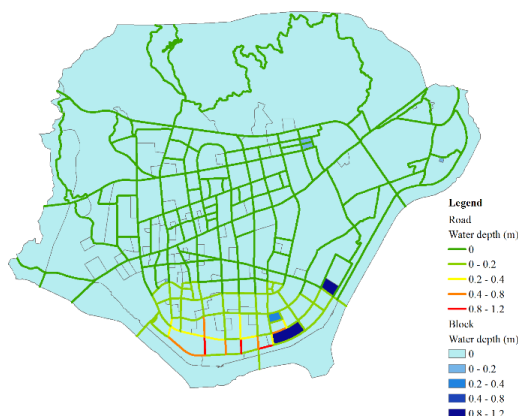


(b) Agent types for disaster scenarios

704 **Figure 8.** Agent types for daily and disaster scenarios.

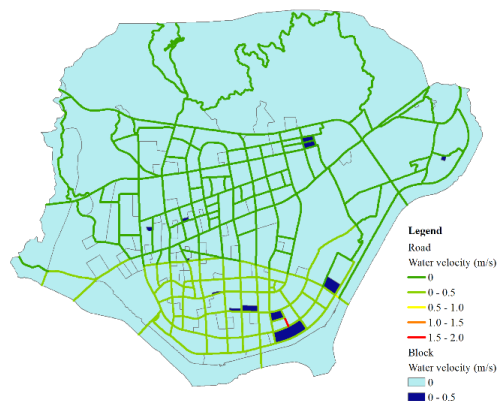


705



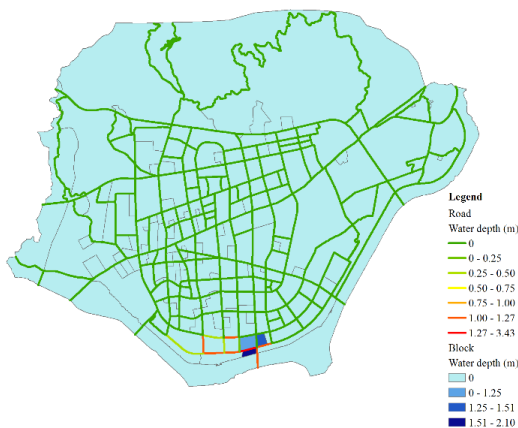
706

(a) Water depth (pluvial flood, T = 15:00)



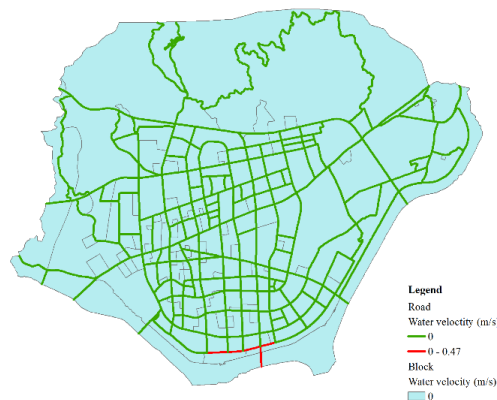
(b) Water velocity (pluvial flood, T = 08:00)

707



708

(c) Water depth (fluvial flood, T = 16:00)



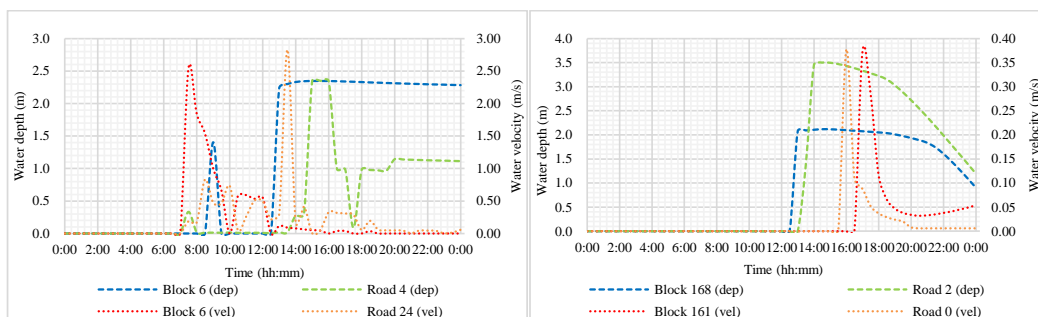
(d) Water velocity (fluvial flood, T = 16:00)

709

Figure 9. Accumulated water depths and velocities. T means time here.



710



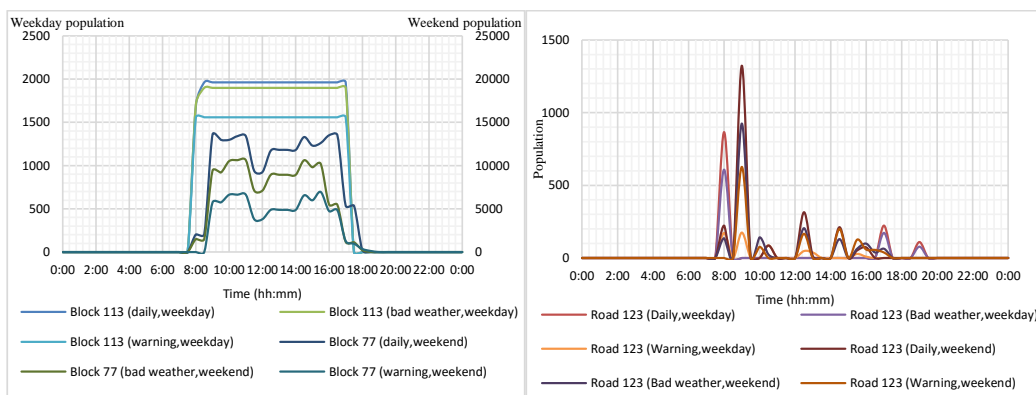
711

(a) Pluvial flood

(b) Fluvial flood

712 **Figure 10.** Changes in the surface water depths and velocities for eight severely flooded areas.

713 The “dep” indicates water depth, and “vel” indicates water velocity.



714

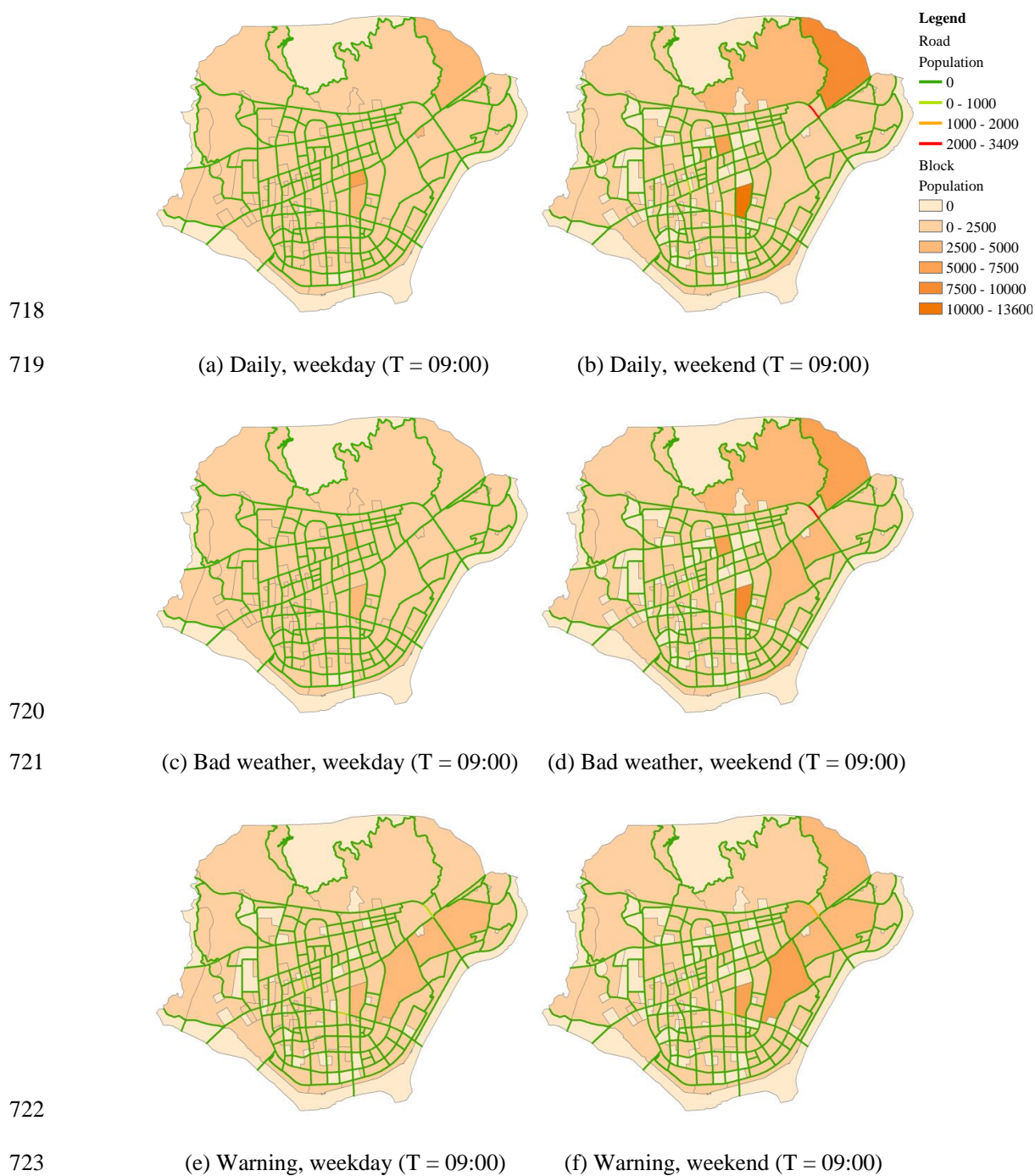
715

(a) Block

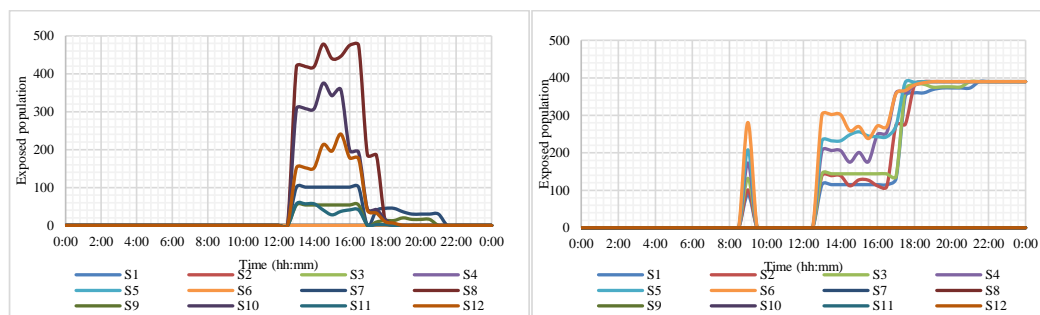
(b) Road

716 **Figure 11.** Population changes in blocks and roads for the six scenarios.

717



724 **Figure 12.** Population distribution for the six scenarios. T means time here.



725

726

(a) Population exposure (Block 168)

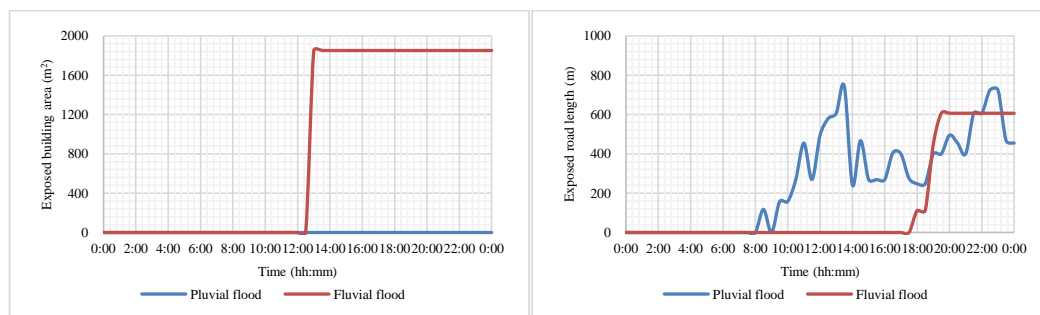
(b) Population exposure (Block 6)

727

Figure 13. Changes in the population exposure of two blocks for the 12 scenarios. Block 168

728

was a recreational area, and Block 6 was a residential area.



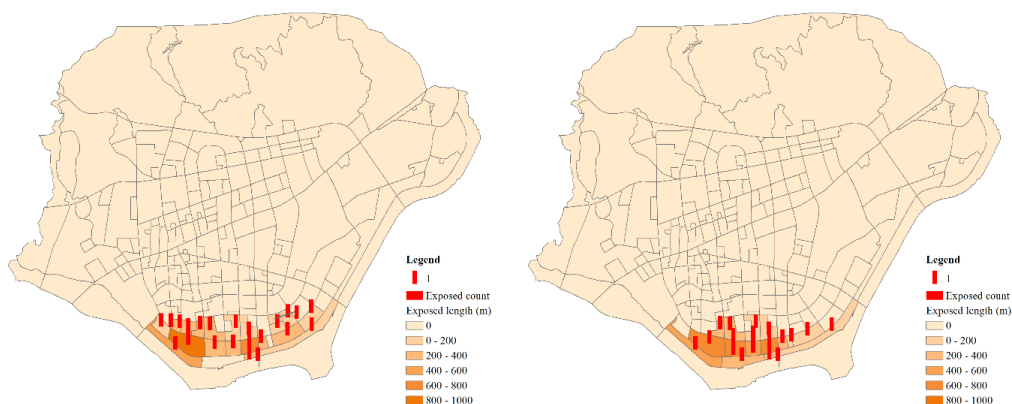
729

730

(a) Exposed building area (Block 168)

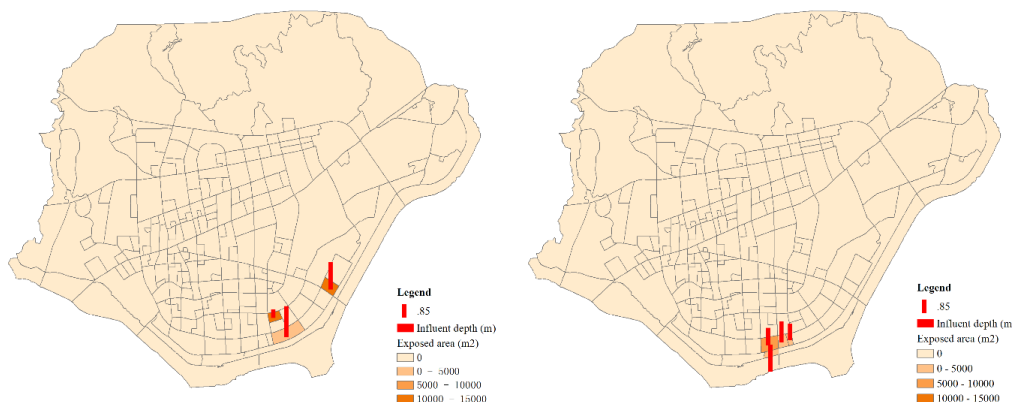
(d) Exposed road length (Block 6)

731 **Figure 14.** Changes in road and building exposures in severely flooded blocks. The exposed road
732 length and building area represent road and building exposures, respectively.



733

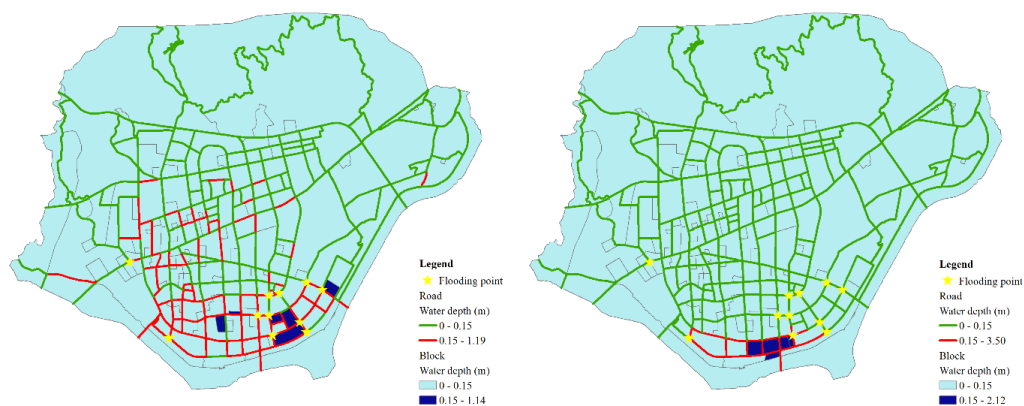
734 (a) Road exposure (pluvial flood, T = 18:30) (b) Road exposure (fluvial flood, T = 18:30)



735

736 (c) Building exposure (pluvial flood, T = 18:30) (d) Building exposure (fluvial flood, T = 18:30)

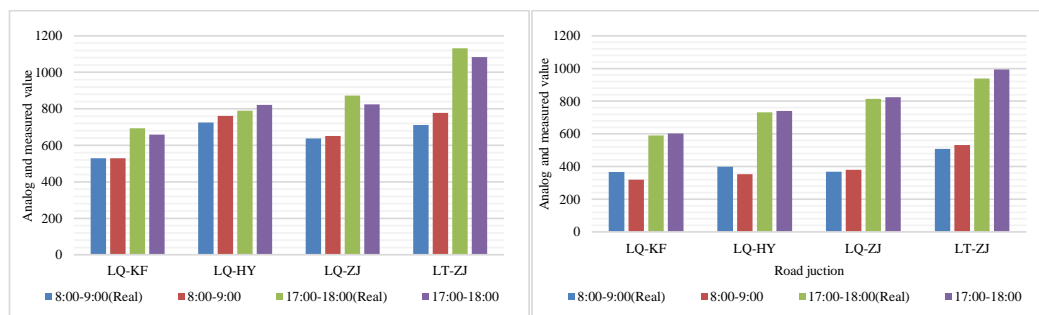
737 **Figure 15.** Map of road and building exposures. T means time here.



(a) Pluvial flood

(b) Fluvial flood

740 **Figure 16.** Map of the flooded area indicating the flooding simulation and the real flood in 2014.
741 The information for the flooded area was provided by Lishui City Housing and Urban-Rural
742 Construction Bureau.



743

744

(a) Weekday

(b) Weekend

745 **Figure 17.** Traffic flow and population simulation results during peak hours on weekdays and
 746 weekends. The traffic flow data were provided by the Lishui City Traffic Bureau. Real means
 747 measured value here. LQ is Liqing Road, KF is Kaifa Road, HY is Huayuan Road, ZJ is Zijin
 748 Road, and LT is Lutang Street.



749 **Table 1** Data used in this study.

750 **Table 2.** Parameter values for the rainstorm intensity formula.

751 **Table 3.** Parameter variations used in the simulation scenarios.

752 **Table 4.** Sociodemographic characteristics of the population in the case study area.

753 **Table 5.** Building step heights for different block types.



754 **Table 1.** Data used in this study.

Data	Source	Time	Use
Digital elevation model	Local government	2013	Topography
Basic geographic data	Local government	2015	Location of river, road and building
Hydrological data	Local government	20 Aug 2014	Flow and water level
1km grid population data	National Earth System Science Data Sharing Infrastructure, National Science & Technology Infrastructure of China (http://www.geodata.cn)	2010	Number of residents in grid of the study area.
Population profile	Lishui Statistical Yearbook and Liandu Yearbook (http://tjj.lishui.gov.cn/sjjw/tjnj/201511/t20151105_448284.htm)	2014	Gender profile, age profile, education level profile, employment profile and travel mode profile were used to classify agent groups.
Traffic flow data	Local government	24 June 2017 to 7 July 2017	The number of vehicles passing through a node within one hour at four intersections from 24 June 2017 to 7 July 2017 in this area,
Water accumulation point	Local government (http://www.zjjs.com.cn/n17/n26/n44/n47/c339697/content.html)	20 Aug 2014	Location

755



756 **Table 2.** Parameter values for the rainstorm intensity formula.

Parameter	Value
A	1265.3
b	5.919
c	0.587
n	0.611

757



758 **Table 3.** Parameter variations used in the simulation scenarios.

Scenarios	Flooding Type	Human behavior	Weekdays or Weekends
S1	Pluvial flood	Daily	Weekdays
S2	Pluvial flood	Daily	Weekends
S3	Pluvial flood	Bad weather	Weekdays
S4	Pluvial flood	Bad weather	Weekends
S5	Pluvial flood	Warning	Weekdays
S6	Pluvial flood	Warning	Weekends
S7	Fluvial flood	Daily	Weekdays
S8	Fluvial flood	Daily	Weekends
S9	Fluvial flood	Bad weather	Weekdays
S10	Fluvial flood	Bad weather	Weekends
S11	Fluvial flood	Warning	Weekdays
S12	Fluvial flood	Warning	Weekends

759

760 **Table 4.** Sociodemographic characteristics of the population in the case study area.

Variables	Groups	Percentage (%)
Gender	Male	50.430
	Female	49.570
Age	0-17	18.730
	18-60	63.340
	>60	17.930
Professional status	Employed	55.770
	Unemployed	44.230
Education Level (Highest diploma)	University, school-college, bachelor	14.457
	No diploma	85.543
Travel mode	Walk	25.24
	Bus	43.06
	Car	31.70

761 Note: The data are from the 2015 Lishui Statistical Yearbook and 2015 Liandu Yearbook.



Table 5. Building step heights for different block types.

No	Block type	Building type	Building steps height
1	Residential area I	Garden house, villa	0.35 m (floors>9, 0.60 m)
2	Residential area II	High-rise apartments and new village houses before and after liberation (before 1988); new residential quarters and commercial houses (after 1988)	0.35 m (floors>9, 0.60 m)
3	Residential area III	New and old Lane homes, three types of staff housing	0.10 m
4	Residential area IV	Shed house	0.05 m
5	School	Educational building	0.35 m (floors>9, 0.60 m)
6	Company	Office building	0.35 m (floors>9, 0.60 m)
7	Recreational area	Public buildings for business, culture, sports and other use	0.35 m (floors>9, 0.60 m)

762